Front. Phys., 2012, 7(5): 521–526
DOI 10.1007/s11467-012-0255-y

RESEARCH ARTICLE

A facile synthesis of branched silver nanowire structures and its applications in surface-enhanced Raman scattering

Feng-Zi Cong[1], Hong Wei[1], Xiao-Rui Tian[1], Hong-Xing Xu[1,2,†]

[1] *Beijing National Laboratory for Condensed Matter Physics and Institute of Physics, Chinese Academy of Sciences, Box 603-146, Beijing 100190, China*

[2] *Division of Solid State Physics/The Nanometer Structure Consortium, Lund University, Box 118, S-22100, Lund, Sweden*

E-mail: †hxxu@iphy.ac.cn

Received June 1, 2012; accepted June 25, 2012

We report a facile method of preparing novel branched silver nanowire structures such as Y-shaped, K-shaped and other multi-branched nanowires. These branched nanostructures are synthesized by reducing silver nitrate ($AgNO_3$) in polyethylene glycol (PEG) with polyvinglpyrrolidone (PVP) as capping agent. Statistical data indicate that for the "y" typed branched nanowire, the branches grow out from the side of the trunk nanowire in a preferential orientation with an angle of 55° between the branch and the trunk. Transmission electron microscopy (TEM) studies indicate that the defects on silver nanowires could support the growth of branched nanowires. Conditions such as the molar ratio of PVP/$AgNO_3$, the reaction temperature, and the degree of polymerization of reducing agent and PVP play important roles in determining the yield of the silver branches. Due to the rough surface, these branched nanostructures can be used as efficient substrates for surface-enhanced Raman scattering applications.

Keywords branched silver nanowire, surface-enhanced Raman scattering (SERS)

PACS numbers 78.67.Uh, 78.30.-j, 78.67.-n, 73.20.Mf

1 Introduction

Intensive investigations have been devoted to the synthesis of metal nanostructures in recent years due to their unique properties which are different from their bulk materials [1, 2]. It has been well-established that the properties of metal nanostructures can be effectively tailored by controlling their size, shape, composition, crystallinity and structure [3–5]. Therefore,they have potential applications in catalysis [6, 7], photonics and plasmonics [8], information technology [9, 10], surface-enhanced Raman scattering (SERS) [11–13], biologic imaging [14], sensing [15–19] and cancer therapy [20, 21]. Within so many different metal nanoparticles that have been intensively investigated, synthesis and study of silver (Ag) nanoparticles are particularly interesting because of their rich optical properties due to the strong surface plasmon resonances (SPRs) in the visible spectral range, which strongly depend on the parameters mentioned above [22]. Accordingly, various shaped Ag nanostructures such as spheres [23], cubes [24], rods [25], rice [26], wires [27], disks [28], triangles [29, 30], rings [31] and prisms [32] have already been synthesized using various methods.

Among all these Ag nanostructures that have been fabricated, the synthesis of branched Ag nanostructures have always attracted people's interests for their high surface to volume ratios and fancy shapes [33–40]. These unique properties make them promising candidates especially when used as catalysts or as substrates for surface-enhanced Raman scattering [34, 35]. So far, the synthesis of such flower-like [33], coral-like [35] and dendritic [36–39] silver nanostructures have been reported. In these structures, some have plenty of short protrusions with length no more than 500 nm [34–37], while others have relatively long protrusions ($>$ 1 mm) [38–40] in which hierarchical nanostructures are prepared by either chemical synthesis or electrochemical deposition. However, to the best of our knowledge, there is still no chemical synthesis of single branched Ag nanowire structures reported.

In this paper, we report for the first time a facile method for the synthesis of single branched silver nanowires as well as multi-branched nanowires. It is

found that the reaction temperature, the polymerization of reducing agent, the degree of polymerization of the capping agent polyvinglpyrrolidone (PVP) and PVP/$AgNO_3$ molar ratio play important roles in the yield of the branched silver nanowire structures. These branches are likely generated by an anisotropic growth from the defects on the surface of silver nanowires observed by TEM. Statistical data indicate that for the "y" typed branched nanowire, the branches grow out from the side of the trunk nanowire in a preferential orientation.

2 Synthesis of branched silver nanostructures

The silver nanobranches were synthesized by a polyol route. Silver nitrate ($AgNO_3$) (purity > 99.8 wt%) and polyvinglpyrrolidone (PVP) with different molecular weight (PVP K30, K50, K90, K130, which means the molecular weight of PVP is 30 kDa, 50 kDa, 90kDa and 130 kDa, respectively) were purchased from Beijing Chemical Reagents Company. Polyethylene Glycol (PEG 200, 600, which means the molecular weight of PEG is 200 Da and 600 Da, respectively) and Ethylene Glycol (EG) were purchased from Guangdong Xilong Chemical Co., Ltd. All reagents were used as received without further purification. Deionized water with resistance of 18 MΩ·cm was used in all cases. In a typical synthesis, 0.1275 g $AgNO_3$ was dissolved in 2.5 mL of 1 M PVP K30 (the concentration was calculated in terms of the repeating unit) aqueous solution, then the whole solution was added into 25 mL PEG 600 in a flask under stirring. The flask was then transferred to an oil bath and heated to make the temperature increase from room temperature to 160°C. The temperature was sustained at 160°C for 30 min. As the temperature rose, the solution first became brown, and then changed to black, and finally dark cyan solution was obtained. After that, the temperature of the oil bath was reduced naturally to 100°C. The solution was kept at 100°C for another ∼4 h, and then cooled in air to room temperature. The purification of the silver nanobranches was conducted by centrifugation. They are separated from the PVP and PEG by centrifugation at 4400 rpm for ∼15 min. The obtained precipitates were then dissolved in deionized water or ethanol and were centrifuged several times in succession. Finally, the sample was dispersed in ethanol for further characterization.

A drop of the suspension was placed on a piece of silicon wafer for scanning electron microscopy (SEM) studies. SEM images were obtained by Hitachi S-4800 and S-5200 scanning electron microscopes. Figure 1 shows low- and high-magnification SEM images of a typical sample. From Fig. 1(a), it can be seen that the final products contain interesting branched nanowires such as Y-shaped [Fig. 1(b)], K-shaped [Fig. 1(c)] and top frame rectangular pyramid like [Fig. 1(d)] nanostructures. Most of these branched nanostructures have a length of about 5–15 μm with each branched part more than 2 μm long and a diameter of ∼200 nm. The Y-shaped ones are the staple products compared with the other branched nanostructures. Besides the branched nanostructures, there are also many irregular nanoparticles in the synthesized products as can be seen from the SEM images in Fig. 1.

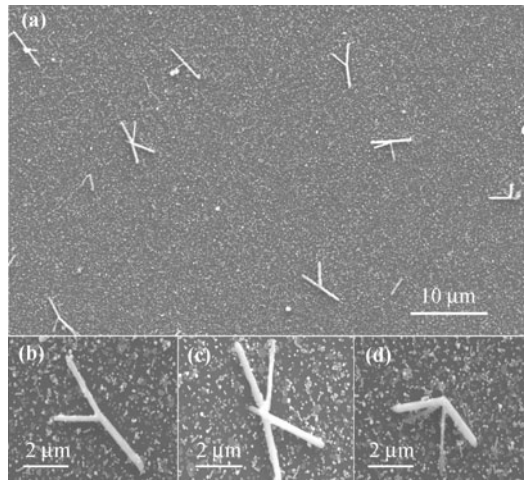

Fig. 1 **(a)** Low- and **(b–d)** High-magnification SEM images of the as-prepared Y-shaped and other branched Ag nanostructures.

The as-prepared Y-shaped nanobranches can be classified into two types. One can be named "$\widetilde{Y}$" type nanobranch [see Fig. 2(a), here we use "$\widetilde{Y}$" to distinguish from "Y" which has already been used to name all the three-terminal nanobranches], with the other named "y" type [see Fig. 2(b)]. Figure 2(c) shows the model of these two types of structures. The angles of these two type nanobranches marked with α and θ in Fig. 2(c) were measured. Figure 2(d) shows the histogram for the angle

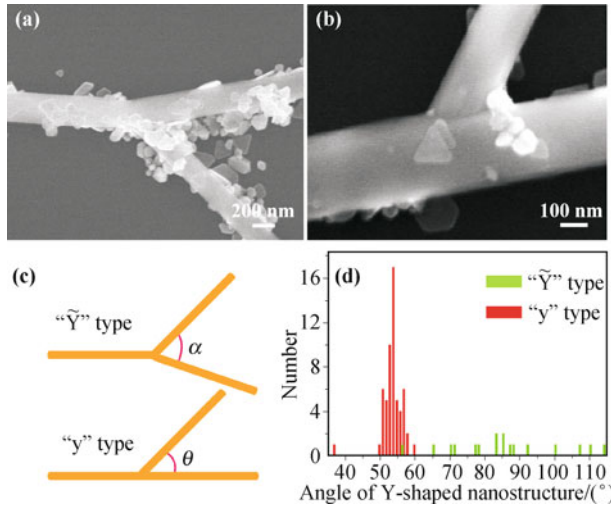

Fig. 2 SEM images of **(a)** "$\widetilde{Y}$" type nanobranch and **(b)** "y" type nanobranch; **(c)** Model of two types of Y-shaped nanobranches; **(d)** Histogram for the angle distribution of the two types of nanobranches. Green bars and red bars represent "$\widetilde{Y}$" type and "y" type, respectively.

distributions of these two types of nanobranches. From the green bars it can be seen that the degree of angles of the "$\widetilde{\text{Y}}$" typed nanobranches are distributed dispersively from 55° to 115°, indicating that no particular degree of angle is evidently preferred. While from the red bars it can be seen that there is a narrow degree distribution concentrated around 55° for "y" typed nanobranch structures, indicating that there is a preferential growth direction for the branches.

3 Growth process of the branched nanowires and discussion of growth mechanisms

Studying the growth process of the branched nanowires could be of help to understand more details in the formation of silver nanobranches. Figure 3 shows SEM images of the products sampled at different time during the formation of the branched nanostructures. When the reactants are heated from room temperature to 160°C and kept heating for ∼30 min in all, Ag nanoparticles with diameter of 50–100 nm are formed first, as can be seen in Fig. 3(a). From that moment on, the heater was set at 100°C and the temperature started to decrease naturally from 160°C. 15 min later,the temperature was at ∼135°C, and the diameter of nanoparticles was increased and nanorods emerged, as is shown in Fig. 3(b). When the whole reaction lasted for ∼60 min, the temperature was nearly reduced to 100°C. At this moment, branched nanostructures appeared such as two linked nanowires [Fig. 3(c)], Y-shaped single-branched structure [Fig. 3(d)] and three-wired nanostructure [Fig. 3(e)]. Then the reactants were kept heating at 100°C for another ∼3 h. Ultimately, the final products had no distinct changes compared with products obtained at ∼60 min, except that larger nanoparticles stuck to the surface of the branched nanowires, making the surface rougher as shown in Fig. 3(f).

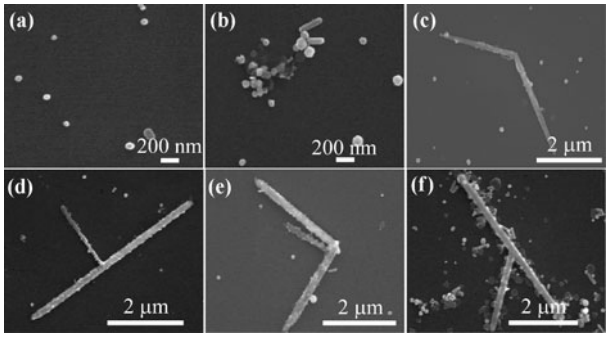

Fig. 3 The SEM images of the products sampled at different time during the synthesis process. **(a)** Sample taken at the moment heated for ∼30 min when the temperature begins lowering; **(b)** Sample taken at the moment when the reactant was heated for ∼45 min, that is, 15 min after the temperature starting to decrease from 160°C; **(c–e)** Samples taken when the reactant was heated for ∼60 min, temperature nearly lowered to 100°C; **(f)** Sample taken when the reactant was heated for ∼4 h, reaction having been finished.

Figure 4 shows the high resolution transmission electron microscopy (TEM) image of a part of an Ag nanowire with a branch. TEM characterization was performed with a JEM-2010 microscope operated at an accelerating voltage of 110 kV. Samples for TEM images were prepared by dropping ethanol solution of the Ag structures on copper grids supported carbon film. From Fig. 4, a relatively ordered crystal lattice (as indicated by the solid black line) can be seen. However, there are local amorphous pattern defects on the surface as marked by arrows in Fig. 4. These defects generated in the growth process of the nanowire branches could function as substrates for the nanoparticles forming and growing by attracting silver atoms added to the surface area of the defects for low surface energy. Thus small nanoparticles were formed on the surface of the nanobranches and grew larger. For the generation of branched nanowires, the capping agent (PVP) could affect the morphological evolution of nanowire structures according to previous studies [41–44]. PVP kinetically controls the growth rates of various facets of silver nanoparticles through preferable adsorption and desorption between the metal surfaces and the functional groups of the capping agent, which leads to anisotropic growth of the nanoparticles. Branched nanowires can be formed by sprouting from defects and growing longer into nanowires at the side of trunk nanowires under the function of PVP. Thus, the most probable growth mechanism is that the defects on the surface of silver nanowires during the initial anisotropic growth trigger another anisotropic growth for

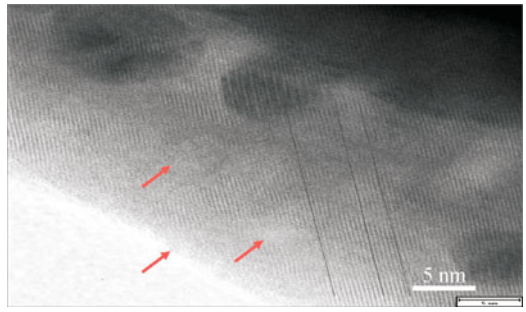

Fig. 4 High resolution TEM image of a part of an Ag nanowire with a branch.

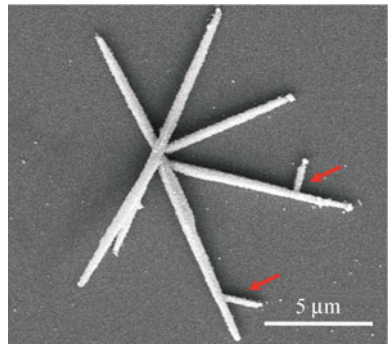

Fig. 5 SEM image of a multi-branched Ag nanowire structure with secondary branches marked by red arrows.

branches. If this mechanism works, more complex branched structures can be grown, which is observed in experiment. Figure 5 shows an example of multi-branched Ag nanowire structures. To reveal in detail the growth mechanisms of the branched nanowires, more detailed high resolution TEM studies are needed [45].

4 Effect of different reaction conditions

The formation of branched nanowires has a strong dependence on the reaction conditions, such as the molar ratio between $AgNO_3$ and PVP, the reaction temperature, the degree of polymerization of reducing agent and capping agent.

By adjusting the molar ratio between the repeating unit of PVP and $AgNO_3$, both the thickness of PVP coating and the location of PVP chains on the surface of a seed could be modified, which in turn, altered the growth of silver nanostructures [46]. The molar ratio between the repeating unit of PVP and $AgNO_3$ was proven to be crucial for the formation of branched nanowires. Here we only changed the amount of $AgNO_3$ to adjust the molar ratio of PVP/$AgNO_3$. When the molar ratio was kept at a typical value of 3.3:1, silver nanobranches were obtained as shown in Fig. 1. However, if the molar ratio was increased to 5:1, only small irregular shaped nanoparticles were obtained. When the molar ratio was decreased to 2.5:1, thicker branched nanowires with more adhered small nanoparticles were synthesized. The diameter of the nanowire was larger than 300 nm. There is no significant morphological difference caused by this small change of molar ratio. Nevertheless, when the molar ratio was continued to decrease to 2:1, irregular nanoparticles and nanorods were obtained, instead of the branched structures. Therefore, it can be concluded that there is a range of value for the molar ratio of PVP/$AgNO_3$ which is suitable for the synthesis of the branched nanostructures. Neither exceeding increase nor decrease of the molar ratio of PVP/$AgNO_3$ is favorable for the formation of silver nanowire branches.

The synthesis of branched nanowires was remarkably influenced by the reaction temperature. When the same reactants were heated at 100°C for ∼4 h, only small nanoparticles and short nanorods were obtained without any branched structures. If the reactants were heated at 160°C for ∼4 h without lowering the temperature, no branched nanostructures were obtained either, except irregular nanoparticles. Therefore, it could be concluded that sufficiently high temperature at the early stage and the temperature falling period are crucial for the formation of branched nanostructures.

By simply changing the degree of polymerization of the reducing agent, the geometries of products could be changed significantly. Lower degree of polymerization was not beneficial to the formation of branched nanostructures. When EG was used as reducing agent, irregular shaped nanoparticles with average diameter of 100 nm were synthesized. When PEG 200 was used as reducing agent, slightly larger nanoparticles were produced. Therefore, no branched nanostructure can be formed by using either EG or PEG 200 as reducing agent.

In the synthesis of branched nanowires, PVP functions as the capping agent. It is found that the degree of polymerization of PVP (n, the average number of repeating units in one PVP macromolecule) plays an important role in determining the yield of branched structures. We tried PVP of several different molecular weights. The molar ratio between the repeating unit of PVP and $AgNO_3$ was 3.3:1 for all these studies in accordance with the typical synthesis. When PVP K58 ($n \approx 520$) and PVP K90 ($n \approx 810$) were used, silver nanoparticles with irregular shapes and sizes were formed. Conglobations of silver nanoparticles were obtained when PVP K130 ($n \approx 11\,700$) was used. Therefore, for the same reaction conditions, higher degree of polymerization of PVP than that of PVP K30 was more likely to form nanoparticles, instead of branched structures.

5 SERS of p-thiocresol on the branched silver nanostructures

Enhanced electromagnetic field can be generated in the junctions between adjacent nanostructures, and the junctions provide the "hot spots" for SERS [47–50]. The branched silver nanowires prepared in this work are attractive for the use as SERS substrates due to the attachment of small particles. To evaluate the performance of the above-mentioned branched silver nanostructures for SERS applications, p-thiocresol was used as probe molecule due to its easy adsorption onto metal nanoparticles [51]. SERS spectra were measured by a confocal Raman spectroscopy system (Renishaw, inVia) equipped with a He–Ne laser which yields the excitation light of 632.8 nm wavelength. The SERS signal was excited and collected through a 100 × objective (NA = 0.85) in a Leica microscope equipped in the Raman system. To get the Raman signal, two long pass edge filters were used to block the laser. An angle-dependent band pass filter was used to select the light centered at 1076 cm^{-1} (± 20 cm^{-1}) for the Raman imaging. The Raman signal for both spectra and images were detected by the CCD camera in the confocal Raman system. By using a beam expander, the diameter of the laser spot is expanded to about 8 μm for the Raman imaging.

Figure 6(a) shows a typical SERS spectrum of the p-thiocresol molecules on a Y-shaped branched nanowire. It is evident that an intense SERS spectrum characteristic of p-thiocresol molecules was obtained with

well-resolved Raman peaks. Figure 6(b) shows bright-field optical images and Raman images of several typical branched nanostructures. The white dashed circles show the size of the laser spot and the white arrows in the Raman images show the polarization of the excitation light. The distribution of the Raman intensity conformably revealed the strong Raman enhancement on the nanobranches within the circular area of excitation. To see clearly the detailed structures of the branched nanowires which were used for SERS detection, SEM measurements were performed. The SEM images of the X-shaped branched nanostructure [Fig. 6(b) iii] are shown as an example in Fig. 6(b) iv and IV. As can be seen, the nanowire surface is covered by plenty of small nanoparticles. The junction between the nanowire and the nanoparticles form the hot spots for Raman enhancement [52]. On the other hand, the aggregates of nanoparticles also form the hot spots. Both kinds of hot spots make these structures favorable for the SERS measurements.

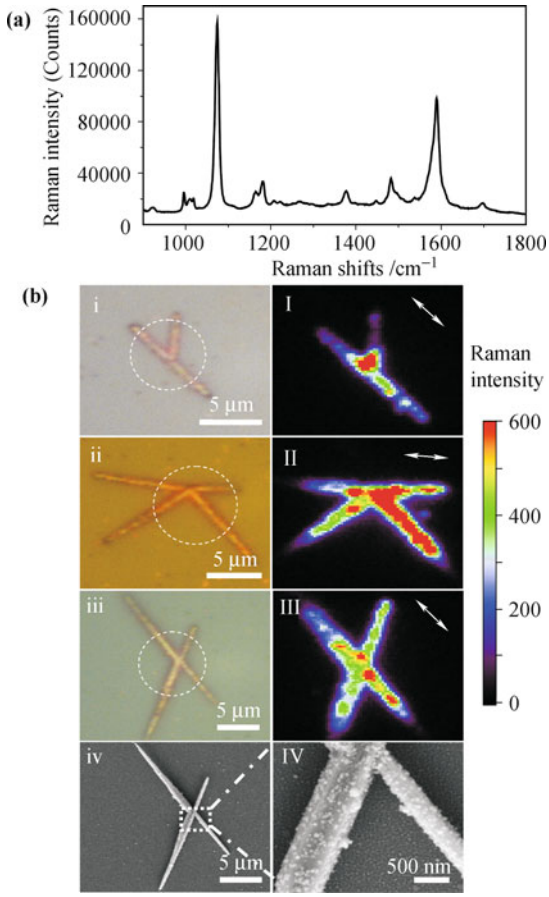

Fig. 6 **(a)** SERS spectrum of p-thiocresol; **(b)** Optical microscope (i, ii, iii) and corresponding Raman images (I, II, III) of three typical branched nanostructures. The white arrows in the Raman images show the polarization of the excitation light. The intensity scale bar is for the Raman images. The white dashed circles show the size of the laser spot, about 8 μm in diameter. iv and IV are the SEM images of the branched nanowire in iii.

Figure 7 shows the polarization dependence measurement of the Raman intensity for the multi-branched nanostructure shown in Fig. 5. The bright-field optical image of this structure is shown in Fig. 7(a). Figure 7(b) shows the Raman images for different excitation polarizations. The Raman enhancement did not show specific dependence on the polarizations of the excitation light. This weak polarization dependence indicates that the rough surface composed of the small nanoparticles play a dominant role in the Raman enhancement effect [53, 54]. In addition, the low sensitivity of the Raman enhancement to the excitation polarization makes the application for SERS detection less restricted to the polarization of the laser light.

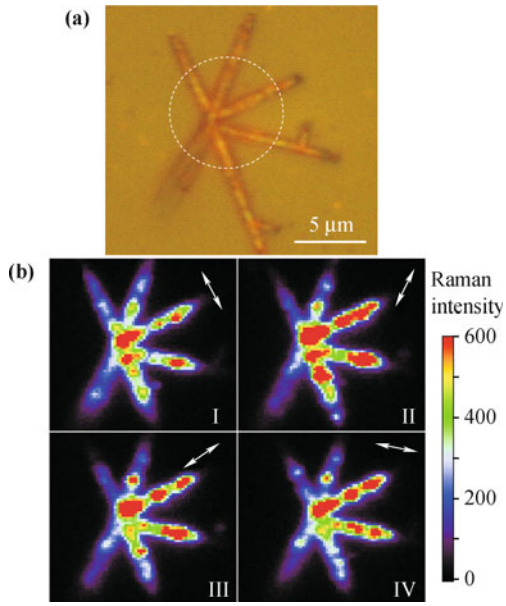

Fig. 7 **(a)** Optical microscope image of a multi-branched nanowire. **(b)** Raman images of the same structure for different incident polarizations. The white arrows show the laser polarization. The white dashed circle shows the size of the laser spot, about 8 μm in diameter.

6 Summary

For the first time the synthesis of novel branched silver nanowires such as Y-shaped, K-shaped, as well as other multi-branched nanowire structures is reported. The synthesis is based on the use of PEG acting as both solvent and reducing reagent and PVP acting as capping agent to reduce $AgNO_3$. These nanostructures can be routinely synthesized with a molar ratio of 3.3:1 between the repeating unit of PVP and $AgNO_3$. The synthesis of the branched nanowire structures is strongly dependent on the molar ratio of PVP to $AgNO_3$, the reaction temperature, the degree of polymerization of both the reducing agent and PVP. Due to their rough surface and micron scale size, these branched nanostructures, which can be easily identified in the optical microscope, are good substrates for surface-enhanced Raman scattering. The Raman enhancement is weakly dependent on the

laser polarization, making these structures show good performance for the excitation light of any polarizations. These branched structures may find potential applications in other fields, for instance catalysis.

Acknowledgements This work was supported by the National Natural Science Foundation of China (Grant Nos. 10625418, 10874233, 11004237, and 11134013), the Ministry of Science and Technology (Grant No. 2009CB930700), and "Knowledge Innovation Project" (KJCX2-EW-W04) of Chinese Academy of Sciences. We thank Prof. Hongyu Chen for helpful discussions.

References

1. Y. N. Xia, P. D. Yang, Y. G. Sun, Y. Y. Wu, B. Mayers, B. Gates, Y. D. Yin, F. Kim, and Y. Q. Yan, Adv. Mater., 2003, 15(5): 353
2. A. R. Tao, S. Habas, and P. D. Yang, Small, 2008, 4(3): 310
3. K. L. Kelly, E. Coronado, L. L. Zhao, and G. C. Schatz, J. Phys. Chem. B, 2003, 107(3): 668
4. S. J. Oldenburg, R. D. Averitt, S. L. Westcott, and N. J. Halas, Chem. Phys. Lett., 1998, 288(2–4): 243
5. C. J. Orendorff, T. K. Sau, and C. J. Murphy, Small, 2006, 2(5): 636
6. R. Narayanan and M. A. El-Sayed, J. Am. Chem. Soc., 2004, 126(23): 7194
7. H. Rashid, R. R. Bhattacharjee, A. Kotal, and T. K. Mandal, Langmuir, 2006, 22(17): 7141
8. N. J. Halas, S. Lal, W.-S. Chang, S. Link, and P. Nordlander, Chem. Rev., 2011, 111(6): 3913
9. H. Wei, Z. P. Li, X. R. Tian, Z. X. Wang, F. Z. Cong, N. Liu, S. P. Zhang, P. Nordlander, N. J. Halas, and H. X. Xu, Nano Lett., 2011, 11(2): 471
10. H. Wei, Z. X. Wang, X. R. Tian, M. Käll, and H. X. Xu, Nat. Commun., 2011, 2: 387
11. H. X. Xu, E. J. Bjerneld, M. Kall, and L. Borjesson, Phys. Rev. Lett., 1999, 83(21): 4357
12. M. Moskovits, J. Raman Spectrosc., 2005, 36: 485
13. Z. Q. Tian, J. Raman Spectrosc., 2005, 36: 466
14. S. Schultz, D. R. Smith, J. J. Mock, and D. A. Schultz, Proc. Natl. Acad. Sci. USA, 2000, 97(3): 996
15. Y. W. C. Cao, R. C. Jin, and C. A. Mirkin, Science, 2002, 297(5586): 1536
16. T. A. Taton, C. A. Mirkin, and R. L. Letsinger, Science, 2000, 289(5485): 1757
17. S. R. Nicewarner-Pena, R. G. Freeman, B. D. Reiss, L. He, D. J. Pena, I. D. Walton, R. Cromer, C. D. Keating, and M. J. Natan, Science, 2001, 294(5540): 137
18. H. X. Xu and M. Kall, Sens. Actuator B-Chem., 2002, 87: 244
19. K. M. Mayer and J. H. Hafner, Chem. Rev., 2011, 111(6): 3828
20. X. H. Huang, I. H. El-Sayed, W. Qian, and M. A. El-Sayed, J. Am. Chem. Soc., 2006, 128(6): 2115
21. S. Lal, S. E. Clare, and N. J. Halas, Acc. Chem. Res., 2008, 41(12): 1842
22. M. Rycenga, C. M. Cobley, J. Zeng, W. Y. Li, C. H. Moran, Q. Zhang, D. Qin, and Y. N. Xia, Chem. Rev., 2011, 111(6): 3669
23. H. Y. Liang, W. Z. Wang, Y. Z. Huang, S. P. Zhang, H. Wei, and H. X. Xu, J. Phys. Chem. C, 2010, 114(16): 7427
24. D. B. Yu and V. W. W. Yam, J. Am. Chem. Soc., 2004, 126(41): 13200
25. H. Y. Chen, Y. Gao, H. R. Zhang, L. B. Liu, H. C. Yu, H. F. Tian, S. S. Xie, and J. Q. Li, J. Phys. Chem. B, 2004, 108(32): 12038
26. H. Y. Liang, H. X. Yang, W. Z. Wang, J. Q. Li, and H. X. Xu, J. Am. Chem. Soc., 2009, 131(17): 6068
27. Y. G. Sun, B. Mayers, T. Herricks, and Y. N. Xia, Nano Lett., 2003, 3(7): 955
28. M. Maillard, P. R. Huang, and L. Brus, Nano Lett., 2003, 3(11): 1611
29. J. T. Zhang, X. L. Li, X. M. Sun, and Y. D. Li, J. Phys. Chem. B, 2005, 109(25): 12544
30. S. H. Chen and D. L. Carroll, Nano Lett., 2002, 2(9): 1003
31. H.-M. Gong, L. Zhou, X.-R. Su, S. Xioo, S.-D. Liu, and Q.-Q. Wang, Adv. Funct. Mater., 2009, 19(2): 298
32. R. C. Jin, Y. W. Cao, C. A. Mirkin, K. L. Kelly, G. C. Schatz, and J. G. Zheng, Science, 2001, 294(5548): 1901
33. X. W. Lou, C. Yuan, and L. A. Archer, Chem. Mater., 2006, 18(17): 3921
34. L. Lu, A. Kobayashi, K. Tawa, and Y. Ozaki, Chem. Mater., 2006, 18(20): 4894
35. Y. L. Wang, P. H. C. Camargo, S. E. Skrabalak, H. C. Gu, and Y. N. Xia, Langmuir, 2008, 24(20): 12042
36. X. G. Wen, Y. T. Xie, M. W. Mak, K. Y. Cheung, X. Y. Li, R. Renneberg, and S. Yang, Langmuir, 2006, 22(10): 4836
37. X. Q. Wang, H. Itoh, K. Naka, and Y. Chujo, Langmuir, 2003, 19(15): 6242
38. J. P. Xiao, Y. Xie, R. Tang, M. Chen, and X. B. Tian, Adv. Mater., 2001, 13(24): 1887
39. J. X. Fang, H. Hahn, R. Krupke, F. Schramm, T. Scherer, B. J. Ding, and X. P. Song, Chem. Commun., 2009, (9): 1130
40. H. Imai, H. Nakamura, and T. Fukuyo, Cryst. Growth Des., 2005, 5(3): 1073
41. Y. G. Sun and Y. N. Xia, Adv. Mater., 2002, 14(11): 833
42. Y. G. Sun, Y. D. Yin, B. T. Mayers, T. Herricks, and Y. N. Xia, Chem. Mater., 2002, 14(11): 4736
43. Y. G. Sun, B. Gates, B. Mayers, and Y. N. Xia, Nano Lett., 2002, 2(2): 165
44. B. Wiley, Y. Sun, and Y. Xia, Acc. Chem. Res., 2007, 40(10): 1067
45. X. C. Jiang, S. X. Xiong, Z. A. Tian, C. Y. Chen, W. M. Chen, and A. B. Yu, J. Phys. Chem. C, 2011, 115(5): 1800
46. B. Wiley, Y. G. Sun, B. Mayers, and Y. N. Xia, Chem. Eur. J., 2005, 11(2): 454
47. H. X. Xu, J. Aizpurua, M. Kall, and P. Apell, Phys. Rev. E, 2000, 62(33): 4318
48. H. X. Xu, Phys. Lett. A, 2003, 312(5–6): 411
49. H. X. Xu, Appl. Phys. Lett., 2004, 85(24): 5980
50. H. Wei, U. Håkanson, Z. L. Yang, F. Höök, and H. X. Xu, Small, 2008, 4(9): 1296
51. J. N. Chen, W. S. Yang, K. Dick, K. Deppert, H. Q. Xu, L. Samuelson, and H. X. Xu, Appl. Phys. Lett., 2008, 92(9): 093110
52. H. Wei, F. Hao, Y. Z. Huang, W. Z. Wang, P. Nordlander, and H. X. Xu, Nano Lett., 2008, 8(8): 2497
53. H. Y. Liang, Z. P. Li, W. Z. Wang, Y. S. Wu, and H. X. Xu, Adv. Mater., 2009, 21(45): 4614
54. B. Zhang, P. Xu, X. M. Xie, H. Wei, Z. P. Li, N. H. Mack, X. J. Han, H. X. Xu, and H. L. Wang, J. Mater. Chem., 2011, 21(8): 2495